An IMU/magnetometer-based Indoor positioning system using Kalman filtering

1 author:

Abdelmoumen Norrdine
Technische Universität Darmstadt
39 PUBLICATIONS   **514** CITATIONS

SEE PROFILE

Some of the authors of this publication are also working on these related projects:

Indoor positioning systems View project

Indoor Localization Systems View project

AN IMU/MAGNETOMETER-BASED INDOOR POSITIONING SYSTEM USING KALMAN FILTERING

Hendrik Hellmers*, Abdelmoumen Norrdine**, Jörg Blankenbach** and Andreas Eichhorn*

*Institute of Geodesy, TU Darmstadt, Germany
Email: {hellmers | eichhorn}@geod.tu-darmstadt.de
**Institute of Geodesy, RWTH Aachen University, Germany
Email: {blankenbach | norrdine}@gia.rwth-aachen.de

Abstract—**Many infrastructure-based indoor positioning technologies such as UWB, WLAN, ultrasonic or infrared are limited by disturbances and errors caused by building objects (e.g. walls, ceiling and furniture). Magnetic fields, however, are able to penetrate various obstacles – in this case commonly used (building) materials – without attenuation, fading, multipath or signal delay. Thus, in the past years a DC Magnetic signal based Indoor Local Positioning System (MILPS), which consists of multiple electrical coils as reference stations and tri-axial magnetic sensors as mobile stations was developed. By observing magnetic field intensities of at least three different magnetic coils, position estimation of the magnetic sensors can be carried out even in severe indoor environments. However, the positioning algorithm currently used is designed for stop-and-go localization.**

This contribution focuses on the integration of a low cost Inertial Measurement Unit (IMU) in order to improve the system's positioning update rate and therefore provide complete 2D localization estimates for kinematic applications and probably afford position solutions even outside the coverage area of MILPS. Therefore an Extended Kalman-Filter (EKF) is adapted for position estimation. The filtering process is accomplished in two steps. The first step leads to position prediction caused by inertial data, which could be updated at the second step by using the MILPS-measurements.

In this context first simulations combining MILPS and IMU have been performed. Testing of the filter with real IMU-data and simulated MILPS positioning data delivered promising results for indoor positioning purposes.

Keywords-component: Indoor-Positioning, Magnetic Fields, Inertial Navigation, Kalman Filter

I. INTRODUCTION

Localization of moving people or objects in severe indoor environments is a very challenging issue. In the last years it is attracting significant interest from both industry and research. A key motivation for this is the growing number of new applications which require for reliable positioning information. Some examples include navigation of travelers in railway stations and airports, guiding of firefighters in dangerous situations or automated robot control within buildings. Main challenges of indoor positioning are the limitations of the technologies available. While many existing indoor localization systems are active assemblies based on methods such as ultrasound, radio or optical waves, each of these has its own assets and drawbacks. The majority of these systems are affected by multi-path fading, temperature and humidity fluctuations, building-related wall and floor attenuation characteristics and the presence of people or moving objects that affect propagation of electromagnetic waves. All these effects will cause different signal degradations that decimate the localization accuracy and availability. In contrast to these methods, magnetic fields are able to penetrate commonly used building materials without attenuation, fading, multipath or signal delay. Thus, the position estimation is not negatively influenced by these interferences. Furthermore, the object to be tracked is equipped with a magnetic field sensor which can be found in conventional smart phones, enabling building-specific location based services. Thus, in the past time a DC Magnetic signal based Indoor Local Positioning System (MILPS) was developed [1-2]. However, depending on the required positioning update rate, which can vary between 1 Hz to less than 0.16 Hz, the reported indoor position accuracies are in the range of few decimeters to several decimeters. This limitation of MILPS is most significant whilst tracking moving objects or persons. In this case the comparatively low update rate leads to distorted trajectories.

To improve the tracking performance (especially the positioning update rate and accuracy) we propose to combine MILPS with a low-cost Micro Electro Mechanical System (MEMS) Inertial Measurement Unit (IMU) consisting of a 3D rate gyroscope and a 3D accelerometer.

Since MILPS has been described in previous papers, in section III a short overview of MILPS will be presented only. After an introduction to Extended Kalman-Filter (EKF) algorithm in Section V, the experimental results of IMU measurement data and simulated MILPS-observations will be presented in section VI and VII, by evaluating the proposed methods with different MILPS update rates. The last section summarizes the presented works and gives a short outlook to future investigations.

II. RELATED WORKS

The challenge of realizing indoor navigation and localization for kinematic applications has been investigated by several authors over the last years [3-11]. The range of commonly used technologies reaches from DC magnetic fields [1-2] and UWB-based systems [3-4] to methods using RFID [5] or WLAN [6]. A short overview of current indoor positioning technologies is shown in [7]. A system for sensor data fusion for localization in indoor environments using various localization principles is given in [8]. Beside these methods also ultrasound [9] or smart phone cameras [10] are also used.

One of the most common technologies is the usage of UWB which allows position estimation based on distance measurements to several reference points. An UWB indoor positioning system based on Kalman-Filter methods are introduced in [3] and [4]. A multi sensor platform containing IMU or GNSS receivers in combination with UWB receiver is given in [11].

Other possible systems consist of WLAN- or RFID-based technologies. Localization of mobile robots in indoor environment using sensor fusion between signal strength identification of WLAN and an IMU is demonstrated in [6]. An RFID/IMU-based system for accurate pedestrian localization is introduced in [5].

A usual processing method is the linear Kalman filter. Because of nonlinearity in commonly used motion equations the Extended Kalman-Filter is used (section V).

III. MILPS – MAGNETIC INDOOR LOCAL POSITIONING SYSTEM

The objective of MILPS is the provision of an accurate and reliable indoor positioning system based on artificial generated magnetic fields covering a whole building with a minimum of infrastructure and complexity. Similar to other infrastructure based systems, reference stations (RS) consisting of magnetic coils are placed inside the building at known positions (X,Y,Z).
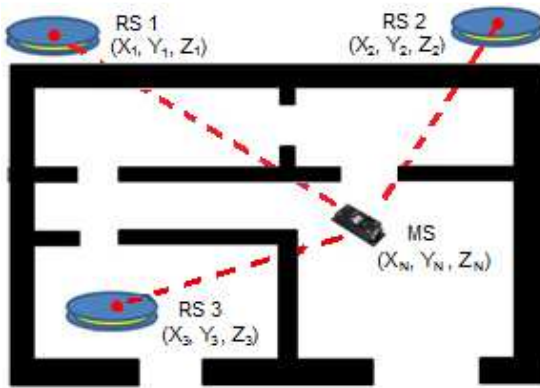

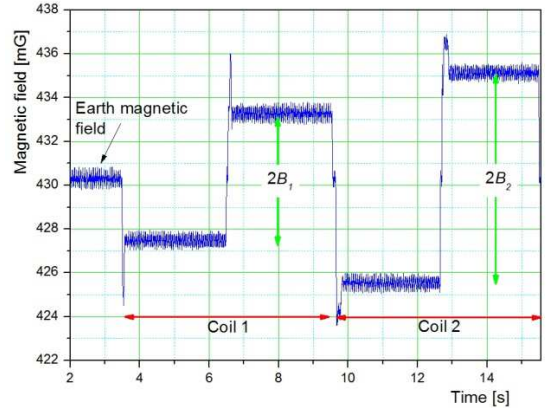Figure 1. Magnetic Indoor Local Positioning System

Figure 2. Captured magnetic field intensity

Capturing the field components of multiple (at least three) coils, the slope distances between the RSi and the Mobile Station (MS) are determinable. Therefore the coordinates (X_{MS}, Y_{MS}, Z_{MS}) can be estimated by use of the trilateration principle. The coils are activated sequentially using real time clock in order to distinguish between their magnetic fields (time division multiplexing, TDM).

IV. SYSTEM OVERVIEW

In previous contributions [1-2] the system has been described which allows the determination of user's 2D or 3D position in indoor areas using magnetic field observations caused by magnetic coils.

Due to the low update rate of the current system, this contribution focuses on the integration of a low cost Inertial Measurement Unit (IMU) in order to improve the system's usability and provide at first 2D localization for kinematic applications even inside areas which are out of MILPS-range. Later therefore the usage of IMU-data enables determination of high rated *dead reckoning* solutions for indoor navigation.

A. Inertial Measurement Unit

In order to determine high-frequency three dimensional positions the ten degree of freedom inertial sensor *ADIS 16480* of *Analog Devices* – consisting of a three axial accelerometer, gyroscope, magnetometer and a digital pressure sensor– was utilized to observe the user's relative motion with a sample rate up to 2.4 kHz. Specific abilities of these sensors are given in Table 1.

Table 1. Abilities of ADIS 16480 [12]

	Acceleration [g]	Gyroscope [°/s]	Magnetometer [mGauss]
Dynamic Range	-10 to 10	-450 to 450	-2.5 to 2.5
Resolution	$1.221 \cdot 10^{-8}$	$3.05 \cdot 10^{-7}$	$1 \cdot 10^{-4}$
Initial Bias Error	0.016	0.2	0.015

According to sample rate f_m the three dimensional acceleration, angular rate and magnetic field are delivered by the IMU. Therefore beside inertial position and orientation it is possible to determine the distances to different reference points by observing the magnetic field of MILPS. This configuration allows an IMU/MILPS integration to get a high-frequency localization updated by absolute solutions derived from external observations by using the method of *Kalman-Filter*.

V.   DATA PROCESSING

Acceleration and angular rates observations of the three-axial IMU sensors are required to achieve high updated two dimensional positioning. For derivation of the system's complete state – consisting of user's position and velocity – at a specific time step, the method of *dead reckoning* is applied.

A. Dead Reckoning

Because in this contribution the user movement is considered in a 2D environment as a first step, only one rotational information (Z-axis) and horizontal accelerations (X- and Y-axis) are needed. Therefore, these observations provide two dimensional position and orientation at every discrete time step in respect to their kinematic. The relation between these measurements and the user's state is described regarding the following known equations [13]:

$$v = \int a \, dt, \tag{1}$$

$$p = \int v \, dt = \iint a \, dt, \tag{2}$$

Where a is the acceleration, v the velocity and p the 2D position. According to the inertial observations depending on time interval Δt these continuous equations have to be transfer into discrete forms [13]:

$$v = a \cdot \Delta t + c_1, \tag{3}$$

$$p = \frac{1}{2} \cdot a \cdot \Delta t^2 + c_1 \cdot \Delta t + c_o, \tag{4}$$

Where p_0 and v_0 describe the initial position and velocity respectively. The state of a system at a time k+1 evolve from the prior state at time k according to the equations

$$p_{k+1} = p_k + v_k \cdot \Delta t + \frac{1}{2} \cdot a_{k+1} \cdot \Delta t^2, \tag{5}$$

$$v_{k+1} = v_k + a_{k+1} \cdot \Delta t. \tag{6}$$

Furthermore the user's current orientation with respect to the sensor frame γ is determined by integrating the horizontal angular rate Ω. For heading estimation in the global frame, an initial orientation γ_0 at k = 0 has to be given [13]:

$$\gamma_{k+1} = \gamma_k + \Omega_{k+1} \cdot \Delta t \tag{7}$$

This orientation is used to estimate the user's propagated position in the global frame by using the two dimensional rotation matrix [14]:

$$\mathcal{R} = \begin{pmatrix} \cos\gamma & -\sin\gamma \\ \sin\gamma & \cos\gamma \end{pmatrix} \tag{8}$$

Considering the rotation matrix (8), equation (5) and (6) can be combined to the following equation of motion for every discrete time step (vectors are illustrated bold) [15]

$$\mathbf{x}_{k+1} = \phi \cdot \mathbf{x}_k + B \cdot \mathcal{R}_{k+1} \cdot \mathbf{u}_{k+1} \tag{9}$$

In this context $\mathbf{x}$ stands for the system's state vector, ϕ for the transition matrix, B for the control matrix, and $\mathbf{u}$ for the current control vector. In detail the different components consist of the following elements:
$\mathbf{x} = (p_x \quad p_y \quad v_x \quad v_y)^T$, where indices x and y represent the coordinate axes.

$$\phi = \begin{pmatrix} 1 & 0 & \Delta t & 0 \\ 0 & 1 & 0 & \Delta t \\ 0 & 0 & 1 & 0 \\ 0 & 0 & 0 & 1 \end{pmatrix}, \tag{10}$$

$$B = \begin{pmatrix} \frac{1}{2}\Delta t^2 & 0 \\ 0 & \frac{1}{2}\Delta t^2 \\ \Delta t & 0 \\ 0 & \Delta t \end{pmatrix} \tag{11}$$

and $\mathbf{u} = (a_x \quad a_y)^T$, where a is the acceleration in one direction. The system's state vector results from integration of velocity and acceleration in respect to Δt (9).

B. Extended Kalman-Filter

Although IMU observations lead to a high-frequency representation of the user's state, dead reckoning solutions are not long-term stable. Beside the specific sensor drift (see Table 1), a linear integration error of acceleration and angular rate affects the result. The neglected nonlinearity of the integration leads to a propagating error rapidely.

To counteract these appearances it is necessary to combine dead reckoning solutions with *position-fixing* supported by an additional system - in this case MILPS. The MILPS-observations are evaluated in combination with a predicted position result from IMU-data by adapting the method of *Extended Kalman Filtering* which is used to continuously update the best estimate of the system's current state [16].
The principle of this operation is to take observations of external distances to one or more reference points into account – in this case magnetic coils – to improve the prediction (9). In the following, predicted states are marked with a superscript minus.

Beside the predicted state vector $\mathbf{x}_k^-$, the predicted variance covariance matrix P_k^- is available for every discrete time step [15]:

$$P_k^- = \phi \cdot P_{k-1} \cdot \phi^T \tag{12}$$

This IMU-data integrated prediction is filtered every time step when MILPS-observations are available. The whole proceeding is described in the following.

At first the nonlinear observation model is expressed by formulating the 2D distance to a specific coil as a function of the user's position:

$$d_i = \sqrt{(X_i - X_n)^2 + (Y_i - Y_n)^2} \tag{13}$$

In this context, n represents the current position and i is one specific reference coil.

Then the *Jacobian matrix* H of d_i is determined with respect to $\mathbf{x}$ [15].

$$H = \left. \frac{\partial d_i(\mathbf{x})}{\partial \mathbf{x}} \right|_{\mathbf{x}=\mathbf{x}_k^-} \tag{14}$$

In general distances to at least two different reference points are necessary for two dimensional position calculations. However, in this case there is no minimum number of external observations since only updates of predicted positions are determined. This filtering process even provides data processing by regarding only one reference point, because MILPS-observations are only used as IMU-data aid (tightly coupled). An increasing number of reference points though, lead to a more accurate solution. Regarding (14) make obvious, that the nonlinear derivations in respect of X- and Y-coordinates have to be linearised by using the predicted position. Because one observed distance depends on a function of positions, the derivations with respect to both velocities v_x and v_y are zero.

Next *Kalman-Matrix* K is computed which is important for the observations' weighting [17]:

$$K = P_k^- \cdot H^T \cdot (H \cdot P_k^- \cdot H^T + R)^{-1} \tag{15}$$

In this equation R stands for the Variance Covariance Matrix (VCM) of the external distance measurements, which includes the MILPS-observations' variances. K serves as a weighting for *innovation* $\mathbf{j}$ which consists of the residuals between measured distance to coil i and the equivalent linearised observation equation:

$$\mathbf{j} = \mathbf{d} - \mathbf{d}(\mathbf{x}_k^-) \tag{16}$$

The estimation update is given by the weighted innovation in addition to the predicted state vector:

$$\hat{\mathbf{x}}_k = \mathbf{x}_k^- + K \cdot \mathbf{j} \tag{17}$$

In this case $\hat{\mathbf{x}}_k$ represents the new estimation for the current state. The corresponding VCM, which consists of the state vector's variances, is given by [17]:

$$\hat{P}_k = (I - K \cdot H) \cdot P_k^- \tag{18}$$

Regarding (17) it becomes apparent that the addition to the predicted state vector only leads to a new approximation of the current state. Because of the system's nonlinearity and the involved linearization it is necessary to execute the filtering process – equation (14) to (17) – iteratively. In this case the calculated state vector (17) provides a current approximation for the next iteration step, which starts with a new updated Jacobian matrix (14). Because of the solution's convergence, the iteration has to be continuing until a preassigned threshold (limiting value) is reached. The filtering process is depicted in Figure 3.
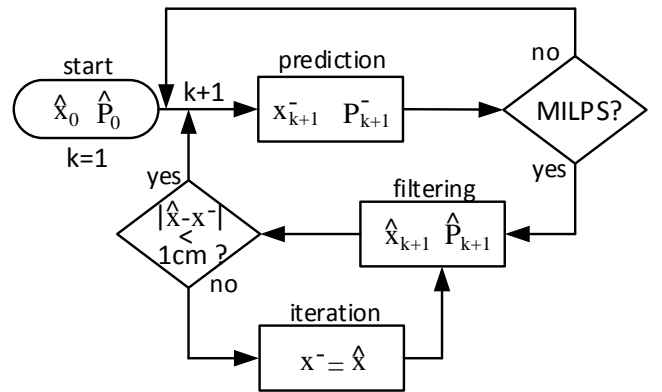

Figure 3. Flow diagram of Kalman-Filter process

VI. POSITIONING

For testing the introduced algorithms of chapter V a test trajectory has been created at the first floor of the institute building, which is shown in Figure 4. Although the method is suitable for providing real time localization, in this test bed data post processing was applied.

The track starts at position 1 and take course around the corridor until it ends at point 13. With a distance of about 3 m positions have been marked at ground floor, so that all track points (from 1 to 13) the trajectory consists of are known in a local coordinate frame. The dashed parts represent inaccessible areas, while the two gaps, which are linked with the corridor, are used for the placements of magnetic coils. In order to get external information about the user's localization, distances between user and coil A and B respectively derived from magnetic field observations are used. For data evaluation according to kinematic applications real reference coils have been utilized but only simulated distance measurements were used in first step.

To observe the motion described by the trajectory's course a small handcart has been used, which consists of a plane surface to install the IMU in a horizontal position (Figure 5).
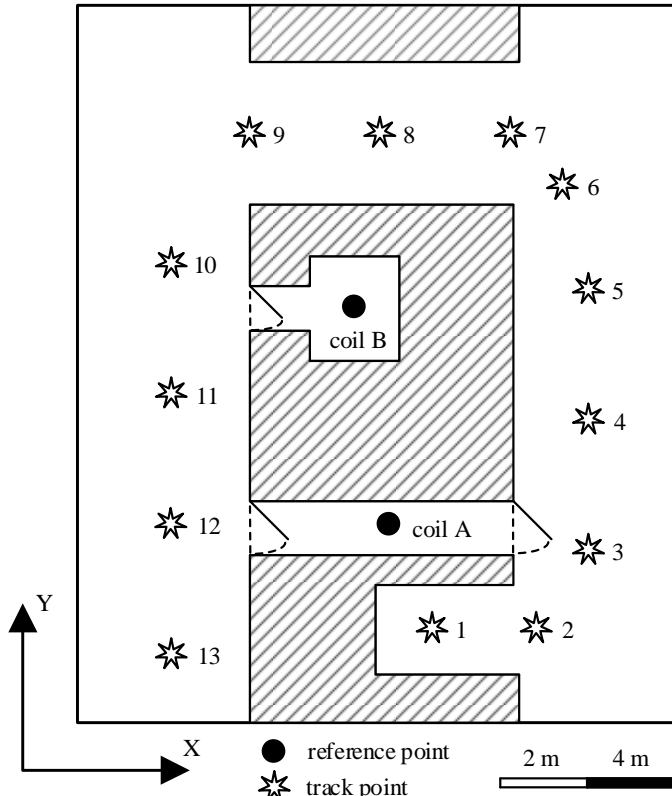
Figure 4. Test bed inside a building

Figure 5. Mobile cart with horizontal IMU

In respect of this initialization the cart has been accelerated and moved along the complete track while observing acceleration and angular rate with a sample rate of 200 Hz to provide a predicted update of position and velocity every 0.005 seconds. To get an acceptable comparison of calculated and true trajectory after data processing, the IMU was marked with a small permanent magnet when passing existing track points.

In order to enable computing state updates calculating by Kalman filtering external distance measurements from MILPS have been simulated every second track point. This is based on an assumption of a specific update rate f_s at both coils. Depending on f_s, the distance measurements can be executed during a known time lag. In present application two different update rates have been examined (chapter VII). Due to the user's movement it is impossible to detect a coil's magnetic field at a constant place. Because of motion the distance to both reference points change with time, so that blurring effects appear. These effects have been taken into account by regarding the user's average velocity and the coil's update rate. Considering these parameters, the covered distance can be computed while observing one specific coil (A or B). This information leads to an estimation of the appeared distance error, so that a defective distance observation can be simulated. In this case the observation to coil A starts at every second track point (3, 5, 7, 9, 11) which follows by observation to coil B. The required time interval of these measurements depends on the coils' update frequencies.

Assuming the distances to both coils refer to the specific track point and the observation starts to coil A, it is evident, that measurements to coil B are affected by a bigger blurring error than to coil A, because the user has been moved away from the starting track point. Additionally to make the observations more realistic, all affected distance observations were added by simulated white Gaussian noise with a variance of about 0.1 m.

A. 2D Dead Reckoning Localization

According to the test environment described above, the covered trajectory has been reconstructed by integrating the two dimensional acceleration and angular rates in respect of time interval $\Delta t = 1/f_m$ regarding (9). In this context the initial heading describes the user's start orientation in the global frame (can be illustrated by regarding building map). Figure 6 shows the reconstructed trajectory using real IMU-data in comparison to the true track. As it can be seen, the calculated course deviates from the true after about two meters of motion from the starting point, because of sensor drifts and integration errors. The bold dots demonstrate estimated positions while passing a track point of the true trajectory. In this way direct comparisons between true and estimated positions could be calculated. In this example the maximum deviation between true and estimated trajectory appears at point 9 with a norm of 7.55 m.
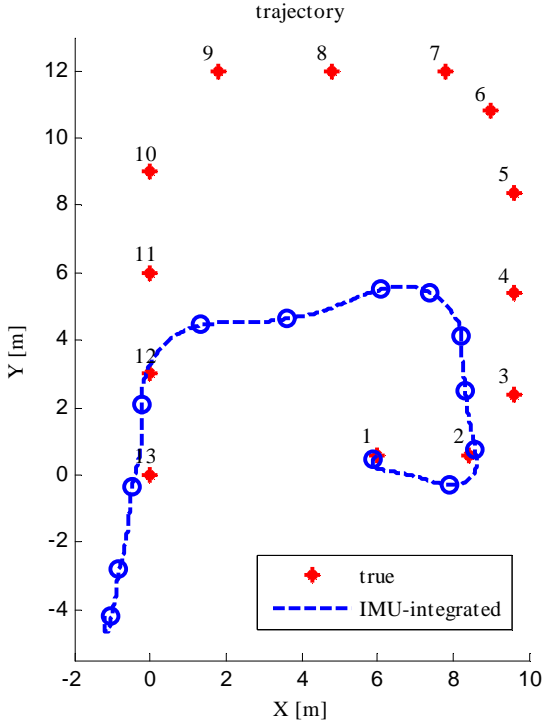
trajectory

Figure 6. IMU-integrated trajectory

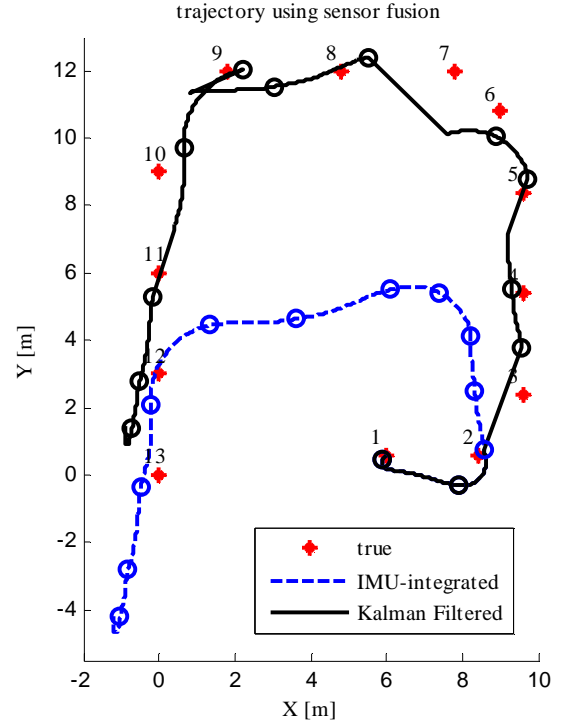trajectory using sensor fusion

Figure 7. Kalman filtered trajectory

B. 2D Localization by Sensor Fusion

To improve the calculated trajectory in respect of the true one external distance measurements have been simulated to support IMU-integrated data by means of Kalman-Filter method. As described above horizontal distance measurements to both reference coils, have been simulated by regarding the true distances and the user's average speed. Because of the observations' dependence of the coils' update interval, two different update frequencies have been compared. The calculated course resulting from a fusion between IMU-integrated data and MILPS-distance measurements is given in Figure 7.

In comparison to the dead reckoning track based on IMU-observations only (dashed curve), the figure shows the calculated trajectory resulting from Kalman filtering. In this case external distance measurements to both reference points have been simulated by assuming an update frequency of 1 Hz at both magnetic coils, which leads to a time interval of about one second to measure one specific distance. The resulting trajectory using position-fixing (in order to improve dead reckoning results) is represented by the continuous curve. The adjusting of the trajectory at points 3, 5, 7, 9 and 11 becomes apparent. In this case a time interval of two seconds is necessary for both observations, which leads to a user's covered distance of about 1.4 m at an average speed of about 0.8 m/s (2.88 km/h).

Although the user's movement causes due to the kinematic unavoidable blurring effects at both measurements it becomes obvious that the true course is represented more accurate by using sensor fusion of both systems. This result confirms the assumption that a data evaluation using a fusion of dead reckoning and position-fixing is suitable for improving the calculated positions.

Equation (15) describes the composition of *Kalman-Matrix* and its dependence on statistic information of both IMU-data and MILPS-observations which are represented in variance covariance matrices P and R. In the evaluation described above the starting statistic model of IMU-observations was represented by using identity matrix, while all external observations from MILPS are assumed as error-free. Therefore all element of R has been set to zero, thus solutions of position-fixing have higher priority.

However regarding the measurement configuration of the external distances, it becomes evident that the observed distance to coil B is more affected by blurring errors than the distance to coil A. In the next step, this statistical information is used at every filtering process which yields a MILPS-measurements variance covariance matrix R unequal to zero. In this case standard deviations of $\sigma_1 = 0.3$ m for distances to coil A and $\sigma_2 = 0.6$ m for distances to coil B are presumed to determine Kalman-Matrix (15).

$$R = \begin{pmatrix} 0.3^2 & 0 \\ 0 & 0.6^2 \end{pmatrix} \qquad P = \begin{pmatrix} 1 & 0 \\ 0 & 1 \end{pmatrix}$$
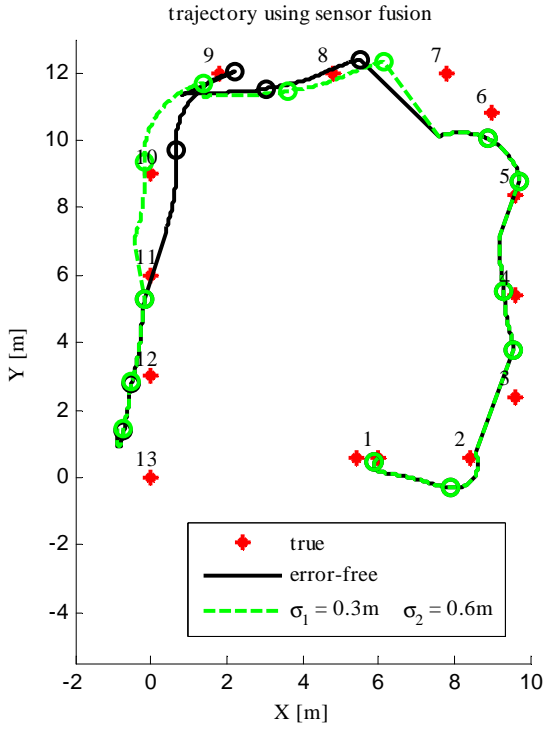
Figure 8. Kalman filtered trajectory using statistical information

As it can be seen an improvement of accuracy at track points 7, 8 and 10 follows by using realistic statistic information to model defective data.

VII. RESULTS

The experiment described first investigations for a hybrid indoor positioning system using sensor fusion. In this case distance measurements from a coil based magnetic positioning system have been simulated and combined with MEMS IMU-data. Therefore two different measurement rates for both coils were applied.

Comparisons of the deviations between true and computed trajectories with respect to different switching intervals are shown in Table 2 and Table 3. Demonstrated are minimal and maximal distances d_{min} and d_{max} between true trajectory and calculated trajectory by considering all track points except the first and the last one.

Table 2. Deviation true and calculated trajectory (1)

Measurement 1	switching interval f_s = 1 Hz	
	d_{min} [cm]	d_{max} [cm]
IMU-integrated	103	755
Error-free	31	230
σ	31	170

Table 3. Deviation true and calculated trajectory (1)

Measurement 1	switching interval f_s = 2 Hz	
	d_{min} [cm]	d_{max} [cm]
IMU-integrated	103	755
Error-free	1	146
σ	29	135

Giving a meaningful statement about the results reproducibility an independent second experiment has been executed (Table 4 and Table 5).

The first row of each table shows minimal and maximal deviation of true and IMU-integrated trajectory. The comparison of Kalman filtered trajectories supported by external distance measurements without regarding statistical information is given in the middle row. Taking into account standard deviations of MILPS-measurements is given at each last row.

The results of these comparisons show a significant improvement of pure dead reckoning solutions by adding information of position-fixing. A maximal deviation between true and calculated trajectory of about 7.5 respectively 4.3 m by using IMU-data only can be reduced to about 1-2 m using sensor fusion. Furthermore an improvement can also be reached by regarding statistical information of MILPS-observations. Obviously an increased update interval leads to more accurate results. While a high update rate reduces the susceptibility of blurring errors, a lower update interval leads to more robust observations.

In addition to Table 4 and Table 5 a comparison of true and calculated trajectories with respect to the deviations of all 13 track points is given in Figure 9 and Figure 10.

Table 4. Deviation between true and calculated trajectory (2)

Measurement 2	switching interval f_s = 1 Hz	
	d_{min} [cm]	d_{max} [cm]
IMU-integrated	54	427
Error-free	40	230
σ	40	230

Table 5. Deviation between true and calculated trajectory (2)

Measurement 2	switching interval f_s = 2 Hz	
	d_{min} [cm]	d_{max} [cm]
IMU-integrated	54	427
Error-free	1	146
σ	7	130
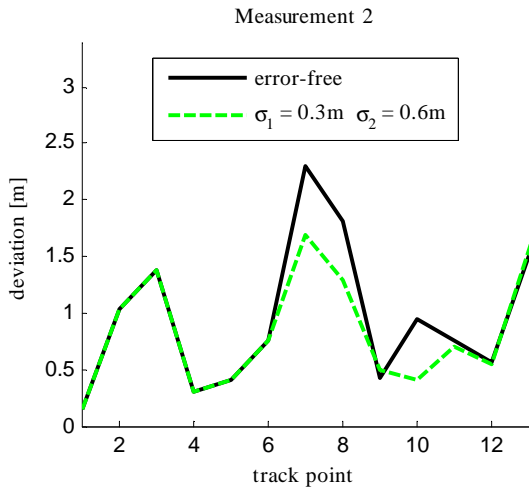
Figure 9. True – calculated (f_s = 1 Hz)
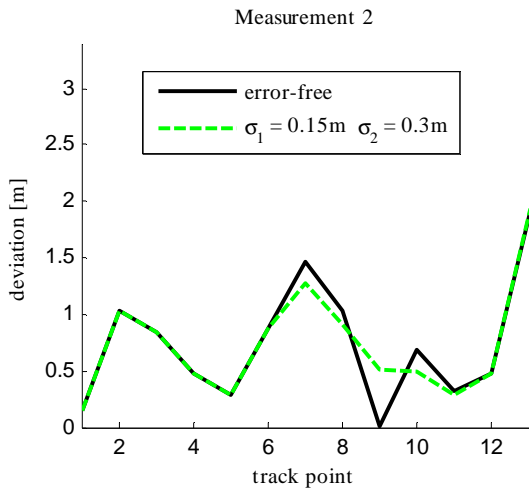
Figure 10. True – calculated (f_s = 2 Hz)

Except from point 9 a similar behavior like measurement 1 can be recognized. External distance observations evaluated by using methods of Kalman-Filter lead to an increasing of the trajectory's accuracy. It is also clear, that significant deviations appear every time after changing direction of movement (point 7 and 10).

VIII. Conclusion and Outlook

In this contribution the aim was to present an indoor positioning system for kinematic applications by using sensor fusion. Because of drifting and non-linearity errors of IMU-integrated data, positioning was supported by using information of an external system. Because of the verified usability of MILPS in indoor environments, this system provides usable solutions for position-fixing. In this case accumulated data were evaluated by using methods of Kalman-Filter.

Distance measurements from MILPS have been simulated assuming two different update intervals. In this case the experimental trajectory has been calculated by using IMU-data and simulated MILPS-observations with a update rate of 1 Hz and

2 Hz. In future works real magnetic field measurements are to be used to find a compromise between decreasing blurring errors and measurements' robustness.

In addition, Kalman filtered trajectories have been evaluated in two different ways using statistical assumptions. At first all MILPS-measurements were assumed to be error-free. At a second step these observations were assumed to be uncertain.

The experimental results have shown that a significant increase of the trajectory's accuracy can be reached by using sensor fusion. The second measurement shows the experiment's reproducibility. This knowledge has to be employed in further works to realize a precise navigation system for kinematic applications in challenging indoor environments. Other examinations will be measurements with changing velocities and more challenging trajectories. Combination of different sensor systems and evaluation using Kalman filtering enables therefore real-time capability.

IX. References

[1] Blankenbach, J., Norrdine, A. und Hellmers, H., A robust and precise 3D indoor positioning system for harsh environments, IEEE Xplore Proceedings of the 2012 International Conference on Indoor Positioning and Indoor Navigation, 13-15 November 2012, Sydney, Australia

[2] Blankenbach J. und Norrdine, A., Position Estimation Using Artificial Generated Magnetic Fields, IEEE Xplore Proceedings of 2010 International Conference on Indoor Positioning and Indoor Navigation, 15-17 September 2010, Zürich, Switzerland

[3] C. Ascher, L. Zwirello, T. Zwick and O.Trommer, "Integrity monitoring for UWB/INS tightly coupled pedestrian indoor scenarios," Indoor Positioning and Indoor Navigation (lPIN), 2011 International Conference on, 2011, pp.1-6

[4] P. Meissner, T. Gigl, and K. Witrisal, "UWB sequential Monte Carlo-positioning using virtual anchors," in Indoor Positioning and Indoor-Navigation (IPIN), 2010 International Conference on, 2010, pp. 1–10

[5] A. Ruiz, F. Granja, J. Honorato, and J. Rosas, "Pedestrian indoor navigation by aiding a foot-mounted imu with rfid signal strength measurements," in Indoor Positioning and Indoor Navigation (IPIN), 2010 International Conference on, 2010, pp. 1–7

[6] V. Malyavej, W. Kumkeaw, M. Aorpimai, "Indoor Robot Localization by RSSI/IMU Sensor Fusion," in Electrical Engineering/Electronics, Computer, Telecommunications and Information Technology (ECTICON), 2013 10th International Conference on, pp. 1-6

[7] Mautz, R. (2012): Indoor Positioning Technologies, Habilitation Thesis at ETH Zurich

[8] L. Klingbeil, M. Romanovas, P. Schneider, M. Traechtler, and Y. Manoli. A modular and mobile system for indoor localization. In Indoor Positioning and Indoor Navigation (IPIN), 2010 International Conference on, pages 1 –10, sept. 2010.

[9] S. Holm, "Ultrasound positioning based on time-of- flight and signal strength," in Indoor Positioning and Indoor Navigation (IPIN), 2012 International Conference on, 2010, pp. 1-6

[10] M. Werner, M. Kessel, and C. Marouane, "Indoor Positioning Using Smartphone Camera," in Proceedings of the 2011 International Conference on Indoor Positioning and Indoor Navigation (IPIN'11), 2011.

[11] A. Kealy et. al., "Collaborative navigation with ground vehicles and personal navigators," Indoor Positioning and Indoor Navigation (IPIN), 2012 International Conference on, 2012, pp. 1-8

[12] Analog Devices, Ten Degres of Freedom Inertial Sensor with Dnamic Orientation Outputs (ADIS 16480), Data Sheet

[13] W. Stolz, Starthilfe Physik, 4. Auflage, Teubner Verlag, Stuttgart 2005

[14] Finkenstein et al., Arbeitsbuch Mathematik für Ingenieure Band I, 4. Auflage, Teubner Verlag, Wiesbaden 2006

[15] J. Wendel, Integrierte Navigationssysteme (Sensorfusion, GPS und Inertiale Navigation), 2. Auflage, Oldenbourg Verlag, München 2011

[16] Eric W. Weisstein, „Kalman Filter". From MathWorld — A Wolfram Web Resource. http://mathworld.wolfram.com/KalmanFilter.html, last accessed July 2013

[17] G. Welch and G. Bishop, "An introduction to the Kalman filter," *University of North Carolina at Chapel Hill, Chapel Hill, NC*, 1995.